Design and Experimental Evaluation of a 2.4 GHz-AoA-Enhanced Beamsteering Algorithm for IEEE 802.11ad mm-Wave WLANs

Avishek Patra, Ljiljana Simić and Marina Petrova
Institute for Networked Systems, RWTH Aachen University
Kackertstrasse 9, D-52072 Aachen, Germany
Email: {avp, lsi, mpe}@inets.rwth-aachen.de

***Abstract*—IEEE 802.11ad millimeter-wave (mm-wave) WLAN nodes achieve high throughput at the cost of the frequent re-steering requirement of highly directional antenna beams to establish and maintain links disrupted by beam misalignment, node mobility, or link blockage. Consequently, rapid and robust beamsteering algorithms are essential to enable seamless communication in mm-wave WLANs. In this paper we propose *AoASteer*, a beamsteering algorithm that speeds up the link establishment process in IEEE 802.11ad mm-wave WLANs by preferentially searching over a subset of mm-wave antenna sectors predicted by 2.4 GHz angle of arrival (AoA) estimation at the access point (AP). We experimentally evaluate the performance of *AoASteer* through extensive measurements in several indoor and outdoor locations, using 60 GHz USRP-SiversIMA packet radio transceivers to gather real mm-wave link information, and a 2.4 GHz USRP-based receiver with an 8-element uniform linear antenna array for AoA estimation, both implemented using GNU Radio. Our evaluation results, obtained for APs with different numbers of beams per sector, show that *AoASteer* typically selects a near-optimal LOS or NLOS link to establish communication, while significantly reducing the link establishment latency. For example, for 4-sector mm-wave antennas, *AoASteer* reduces the latency by 46 μs for 73% of our measurement cases compared to the IEEE 802.11ad beamsteering algorithm, while achieving the highest data rate of 6.7 Gbps for 92% of the cases.**

I. Introduction

Directional antennas in mm-wave networks mitigate the high attenuation inherent at such high frequencies. However this makes the mm-wave link establishment process complex as the antennas must be precisely steered to specific orientations to successfully establish a link. The process of aligning the antenna orientations of two nodes to establish a link between them is called *beamsteering*. In addition to initial link establishment, beamsteering algorithms are responsible for maintaining connectivity through rapid re-establishment mechanisms. Considering that mm-wave links are easily disrupted by slight beam misalignment [1], node mobility [2] or link blockage [3], robust and fast algorithms are essential for seamless communication. The state-of-the-art beamsteering algorithm in the IEEE 802.11ad standard [4], adopted for mm-wave WLANs operating at 60 GHz, is essentially a breadth-first search algorithm. In IEEE 802.11ad, the antenna radiation pattern is divided into wide beamwidth *sectors*, each comprising of multiple narrow, high gain *beams*. For beamsteering, the algorithm first sequentially scans over all sectors to obtain the best sector of a node, followed by scanning through the best sector beams to select the best beam for link establishment. Such exhaustive scanning induces high latency that significantly reduces QoS in mm-wave WLANs.

In this paper, we present *AoASteer*, a fast beamsteering algorithm for IEEE 802.11ad mm-wave WLANs which utilizes 2.4 GHz angle-of-arrival (AoA) estimation to quickly establish a link between 60 GHz nodes. Using *AoASteer*, an access point (AP) equipped with an antenna array estimates the AoA of the 2.4 GHz signal from a user equipment (UE), based on which a subset of feasible 60 GHz AP sectors is predicted. We use this *estimated* AP sector subset to then determine the best sectors and beams of the AP–UE pair for link establishment. We define the messaging protocol for *AoASteer* in detail, and present the results of an extensive experimental evaluation in several indoor and outdoor locations. For our measurements, we employ 60 GHz USRP-SiversIMA packet-radio transceivers and a 2.4 GHz USRP-based receiver with an 8-element uniform linear array (ULA) antenna. Our results show that *AoASteer* significantly reduces the link establishment latency compared to the IEEE 802.11ad beamsteering algorithm while typically achieving the optimal data rate over the link.

A number of mm-wave beamsteering algorithms have been proposed in the literature [1], [5], [6], [7], [8], [9]. The solution in [5] utilizes the correlation between the mm-wave links of two nodes to predict their quality when one link experiences degradation. The proposal nevertheless depends on extensive scanning to determine the links between the nodes. In [6], optimal AP-UE re-deployment positions are chosen by predicting the links at unobserved spots to prevent link blockage. However, the underlying assumption of re-deployment of nodes, especially APs, is not practically feasible. In the algorithm proposed in [7], the orientation receiving the highest signal energy is chosen as the beamsteering direction. While promising, the work proposes no mechanism for node coordination. Additionally, energy detection along multiple directions may lead to increased latency. Solutions

978-1-5386-2723-5/17/$31.00

utilizing information from *non*-mm-wave band signals have been proposed in [8], [9], where the proposed algorithms exploit 2.4/5 GHz Wi-Fi received signal strength (RSS) to predict possible mm-wave beamsteering directions. Although these approaches are promising for static networks, they may not work for dynamic networks given the need of databases for Wi-Fi fingerprints and best mm-wave beam IDs.

The idea of using out-of-band AoA information for beamsteering in mm-wave networks was first introduced in [1], where the authors demonstrated the possibility of predicting line-of-sight (LOS) mm-wave links using AoA estimation of a 2.4 GHz signal. However, this work focused only on LOS links for link establishment, with a limited proof-of-concept experimental evaluation, conducted solely in a single simple indoor environment. By contrast, the AoA estimation system in our work can distinguish multiple LOS *and* non-LOS (NLOS) signals in the horizontal plane and therefore, even under LOS blockage conditions, *AoASteer* can establish connectivity via a NLOS link. Additionally, only the upper bound on the link establishment latency is provided in [1] for a single fixed sector/beam configuration, assuming perfect sector prediction accuracy. In our work, we instead present a detailed experimental evaluation of latency reduction using *AoASteer*, via extensive measurements in several diverse indoor and outdoor locations. We also consider different numbers of sectors per mm-wave antenna, thus studying the influence of the antenna configuration on *AoASteer*'s performance. Finally, in [1] the 2.4 GHz signal AoA is estimated at both the AP and the UE. We argue that 2.4 GHz AoA estimation at the UE is unrealistic in practice, given the large size of a 2.4 GHz receiver array. Therefore, *AoASteer* obtains AoA information at the AP only.

The rest of the paper is organized as follows. In Sections II and III, we detail beamsteering in IEEE 802.11ad and *AoASteer*. The *AoASteer* performance bound are presented in Section IV. We present our evaluation methodology and results in Sections V and VI. We conclude our work in Section VII.

II. IEEE 802.11AD BEAMSTEERING ALGORITHM

In Figs. 1a and 1b, we illustrate the *Sector Level Sweep (SLS)* and *Beam Refinement Phase (BRP)* operations for the IEEE 802.11ad beamsteering algorithm [4]. The SLS phase determines the best sectors of the nodes, whereas the antenna configurations are fine-tuned in the BRP phase to obtain the best beams in the best sectors selected in the SLS phase. The SLS phase begins with the *initiator sector sweep* in which the initiator (i.e., the AP) transmits Sector Sweep (SSW) frames – containing the transmission sector ID in the `SectorID` field and a countdown value indicating the number of remaining SSW frames in the `CDOWN` field – sequentially along its sectors while the responder (i.e., the UE) listens quasi-omnidirectionally. A SSW frame is successfully delivered if the RSS at the responder is greater than the minimum receiver sensitivity threshold, λ. Depending on the initiator sectors that successfully deliver SSW frames, the responder then selects the best transmit sector of the initiator, S_{SLS}^{AP} (i.e., the initiator sector for which the RSS at the responder is highest). The end of the initiator sweep triggers the *responder sector sweep*. These SSW frames transmitted by the responder additionally contain information for the best transmit sector of the initiator in the `BestSector` field. Once the responder sweep is over, the initiator reports the best transmit sector, S_{SLS}^{UE} of the responder through a SSW Feedback frame. An SSW ACK frame from the responder indicates the end of the SLS phase. The BRP phase may be initiated by either of the nodes via a SSW ACK or a BRP frame. For example, in Fig. 1a, the responder initiates the BRP phase by requesting for a *responder receive training* for its best sector. The request is made by setting the `L-RX` field of the SSW ACK frame to $|\mathbf{N}|/4$, where $|\mathbf{N}|$ is the number of beams in each responder sector. Accordingly, the initiator responds with a BRP frame with $|\mathbf{N}|$ appended training subfields. The responder receives the BRP frame sequentially along the $|\mathbf{N}|$ beams of S_{SLS}^{UE}. In the same BRP frame, the initiator also requests an *initiator receive training* and is similarly responded to by the responder with a BRP frame with attached training subfields. On completion of the BRP phase, the best beam pair, $\{S_{SLS}^{AP}{:}B_{best}^{AP}, S_{SLS}^{UE}{:}B_{best}^{UE}\}$ is determined.

III. AOASTEER BEAMSTERING ALGORITHM

In this section, we present the design of our proposed beamsteering algorithm, *AoASteer*. *AoASteer* reduces the link establishment latency by using a *short* SLS (S-SLS) phase (Fig. 1c) based on 2.4 GHz AoA estimation to predict 60 GHz AP sectors. The IEEE 802.11ad BRP mechanism is then used to search for the best beam within the best AP sector found in the S-SLS phase. Accordingly, we assume the 60 GHz nodes to be equipped with a 2.4 GHz radio front-end, with the AP also fitted with a 2.4 GHz antenna array for AoA estimation.

To establish a link, the UE transmits request beacons omnidirectionally over the 2.4 GHz channel. On receiving the request beacons, the AP estimates the AoA of the 2.4 GHz signal using the MUSIC-based AoA estimation algorithm presented in Section V-B. Once the AoAs (denoted by $\hat{\phi}$) are estimated from the MUSIC spectrum, a function Q(.) maps them to the nearest 60 GHz AP sectors. We thereby estimate a subset of feasible AP sectors, $\mathbf{m}$ (corresponding to the $|\mathbf{m}|$ strongest AoAs in $\hat{\phi}$) out of all AP sectors, $\mathbf{M}$ ($|\mathbf{m}| \leq |\mathbf{M}|$). Once estimated, *AoASteer* initiates the S-SLS phase during which the initiator (AP), instead of transmitting SSW frames via all $|\mathbf{M}|$ sectors as in IEEE 802.11ad SLS, transmits only via the subset of estimated AP sectors $\mathbf{m}$. Accordingly, `CDOWN` is set to $|\mathbf{m}| - 1$ for the 1^{st} initiator SSW frame and it counts down to 0 for the $|\mathbf{m}|^{th}$ frame. When transmissions from all $|\mathbf{m}|$ sectors are complete, the initiator switches to quasi-omnidirectional reception mode, listening for the duration of T_{out}. During the initiator sweep, the responder (UE) listens quasi-omnidirectionally over the 60 GHz channel. If at least 1 SSW frame is successfully received, the responder computes the best initiator sector, $S_{S-SLS}^{AP,est}$ from all the received SSW frames. The responder then triggers a responder sector sweep on completion of the initiator sweep to report back $S_{S-SLS}^{AP,est}$ to the initiator. Given

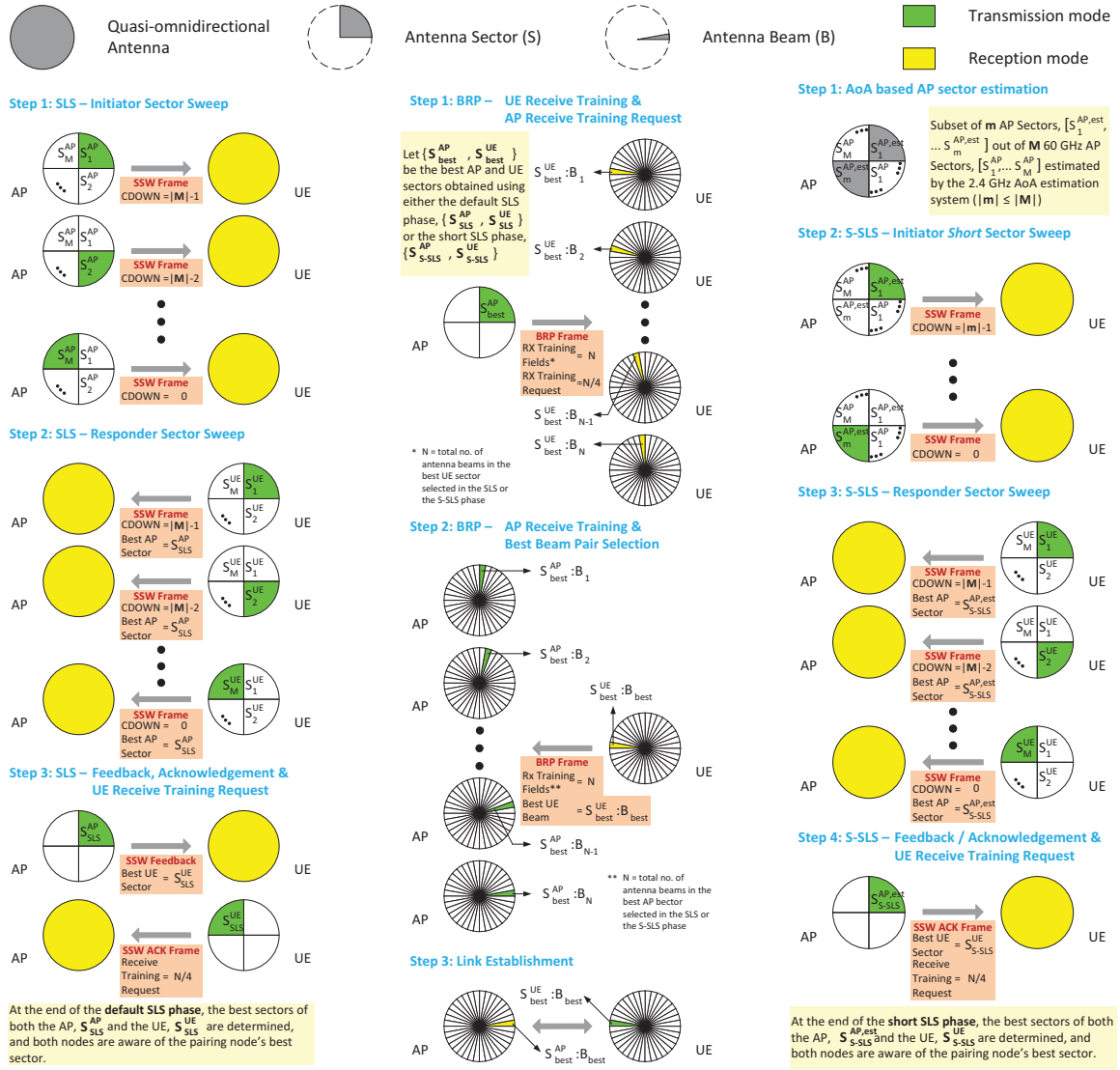

(a) Default SLS (b) Default BRP (c) Short SLS for *AoASteer*

Fig. 1: Example Sector Level Sweep (SLS) and Beam Refinement Phase (BRP) operations for the default IEEE 802.11ad beamsteering algorithm and the proposed Short Sector Level Sweep (S-SLS) phase operations for *AoASteer*.

that we only pre-select sectors for the initiator, SSW frames are transmitted by all $|\mathbf{M}|$ sectors in the responder sweep. Along with reporting the best initiator sector, responder SSW frames also indicate successful delivery of SSW frames during the initiator sweep. We set the initiator reception duration, T_{out}, to the duration required to transmit $|\mathbf{M}|$ SSW frames from the responder. At the end of the responder sweep, the initiator extracts the best initiator sector, $S^{AP,est}_{S-SLS}$, and computes the best responder sector, S^{UE}_{S-SLS}. A single SSW Feedback frame reports back S^{UE}_{S-SLS} to the responder while also requesting for a responder receive training for the $\mathbf{N}$ beams of S^{UE}_{S-SLS} in the BRP phase. At the end of S-SLS, the BRP mechanism defined in Section II is triggered. On completion, we obtain the best beam pair, $\{S^{AP,est}_{S-SLS}{:}B^{AP,est}_{best}, S^{UE}_{S-SLS}{:}B^{UE}_{best}\}$ for link establishment. In case the initiator does not receive a responder SSW frame within T_{out}, indicating that none of the $|\mathbf{m}|$ estimated AP sectors were valid, the initiator falls back to the default IEEE 802.11ad algorithm (the $\mathbf{m}$ AP sectors already tested during S-SLS are *excluded* from SLS).

IV. Performance Bounds

In Fig. 2, we present the link establishment latency bounds for *AoASteer* and the IEEE 802.11ad beamsteering algorithm. For *AoASteer*, we present the best-case performance, i.e. the lowest achievable latency computed assuming perfect estimation of feasible AP sectors, for $|\mathbf{m}|$ = 1, 2 and 3 estimated AP sectors. Additionally, the latencies are computed for different numbers of sectors per node antenna, $|\mathbf{M}|$. The equations for latency computation for the SLS, BRP and S-SLS phases are given by (1), (2) and (3) respectively, where the different frame

TABLE I: FRAME TRANSMISSION AND IFS DURATIONS

SSW Frame (T_{SSW})	14.8 μs	Training field	
SSW Feedback (T_{FB})	15.4 μs	(T_{train})	2.84 μs
SSW ACK (T_{ACK})	15.4 μs	$SBIFS$	1 μs
BRP Frame (T_{BRP})	12.3 μs	$MBIFS$	9 μs

transmission and inter-frame spacing durations, considered in accordance with the IEEE 802.11ad standard, are listed in Table I. Assuming that we correctly predict 1 feasible AP sector for $|\mathbf{m}| = 1$, we observe that *AoASteer* outperforms the IEEE 802.11ad beamsteering algorithm by reducing the link establishment latency by 19% to 40% (obtained for $|\mathbf{M}| = 2$ and 9 respectively). Such a reduction is achieved by shortening of the SLS phase responsible for selecting best sectors of a node from all $|\mathbf{M}|$ sectors. Consequently, we observe higher latency reduction with the increase in $|\mathbf{M}|$. From Fig. 2, we also observe that incrementing $|\mathbf{m}|$ by 1 increases the latency by 4%-7%. Nonetheless, the overall latency for $|\mathbf{m}| = 2$ and 3 still remains lower than the IEEE 802.11ad latency. Therefore, given the possibilities of false estimation of AP sectors using *AoASteer*, we expect $|\mathbf{m}|$ greater than 1 to perform better for inaccurate AP sector estimation conditions.

We note that in practice, $|\mathbf{M}|$ must be selected considering the tradeoff between the link establishment latency (lower for small $|\mathbf{M}|$) and the discoverability of the directional mm-wave links (fewer weaker directional mm-wave links are discovered with the lower gain sectors for small $|\mathbf{M}|$). Therefore, although the best sectors can be selected faster in the SLS/S-SLS phase for nodes with fewer antenna sectors, the reduced gains[1] for these wider sectors may result in the misdetection of sectors with highly directional, feasible beams. This relationship between $|\mathbf{M}|$ and the percentage of available feasible links[2] discoverable is shown in Fig. 2. Therefore, the antenna configuration must be selected considering the tradeoff between the latency reduction and link discoverability. Moreover, given the emerging status of mm-wave beamforming antennas, the production feasibility of arbitrary sector/beam configurations for the antennas is uncertain. Therefore, our link establishment latency study for *different* numbers of sectors per node, $|\mathbf{M}|$ is of considerable academic and engineering interest.

V. EXPERIMENTAL EVALUATION METHODOLOGY

We experimentally evaluated the performance of *AoASteer* through measurement-based link establishment emulation. We

[1]We calculated the sector gains using equation (2-51) in [10] and considering our 10° horn antenna with directional gain 25 dBi and the emulated quasi-omnidirectional antenna of gain 10 dBi as the reference (Section V-A).

[2]The percentage of available feasible links discoverable for different values of $|\mathbf{M}|$ are empirically computed for 60 GHz measurements from several locations as presented in Figs. 3 and 4, and elaborated in Section V.

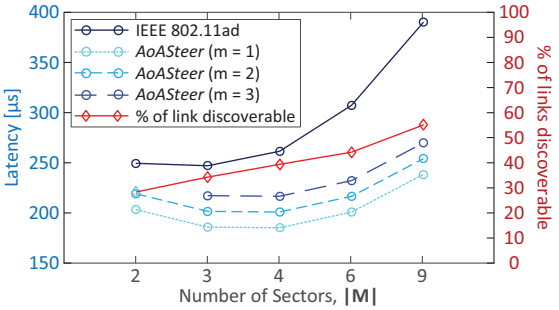

Fig. 2: Link establishment latency for *AoASteer* (best-case) and the IEEE 802.11ad beamsteering algorithm, and the percentage of feasible links discoverable for different number of antenna sectors.

TABLE II: 60 GHZ AND 2.4 GHZ MEASUREMENT SCENARIOS

Indoor	*RX-TX*	Δ*Height*	**Outdoor**	*RX-TX*	Δ*Height*
IN1	A–B	–	OUT1	I–J	–
IN2	A–C	–	OUT2	I–J	0.8 m
IN3	A–D	–	OUT3	K–L	1.2 m
IN4	E–F	–	OUT4	K–M	0.4 m
IN5	E–G	–	OUT5	N–P	–
IN6	E–H	–	OUT6	N–Q	0.5 m

conducted AoA and RSS measurements for 2.4 GHz and 60 GHz signals, respectively, in several indoor and outdoor locations as listed in Table II and shown in Figs. 3 and 4. For the 2.4 GHz measurements, we deployed an AP and a UE at each locations, with the AP operating in reception mode to estimate the AoA of the signal transmitted by the UE. *AoASteer* uses this AoA information to *estimate* a subset of 60 GHz AP sectors for fast link establishment. To verify the estimation accuracy, we conducted 60 GHz measurements for the same AP–UE locations. From the 60 GHz measurements, we obtain the RSS at the UE for transmissions from the AP. This allowed us to determine the actual set of feasible 60 GHz links between the nodes and thereby, extract the set of 60 GHz AP sectors that enable link formation. For 60 GHz measurements, we assume reciprocity of the links such that the RSS at the UE is equal to the RSS at the AP for the given node locations and beam pair. We then evaluated the validity of the subset of 60 GHz AP sectors predicted by the 2.4 GHz AoA estimation system by comparing them with the set of actual feasible 60 GHz AP sectors obtained via the 60 GHz measurements. Depending on the 60 GHz AP sector prediction accuracy, we then computed the link establishment latency using *AoASteer* and the IEEE 802.11ad beamsteering algorithm in MATLAB. In the rest of this section, we first present the 60 GHz transceiver and the 2.4 GHz AoA estimation systems, followed by our evaluation metrics.

$$\textit{SLS duration} = \big[|\mathbf{M}| \times (T_{SSW} + SBIFS) + MBIFS\big] \times 2 + T_{FB} + MBIFS + T_{ACK} + MBIFS \quad (1)$$

$$\textit{BRP duration} = \big[T_{BRP} + |\mathbf{N}| \times T_{train}\big] + SBIFS + \big[T_{BRP} + |\mathbf{N}| \times T_{train}\big] \quad (2)$$

$$\textit{S-SLS duration} = \big[|\mathbf{m}| \times (T_{SSW} + SBIFS)\big] + MBIFS + \big[|\mathbf{M}| \times (T_{SSW} + SBIFS)\big] + MBIFS + T_{ACK} + MBIFS \quad (3)$$

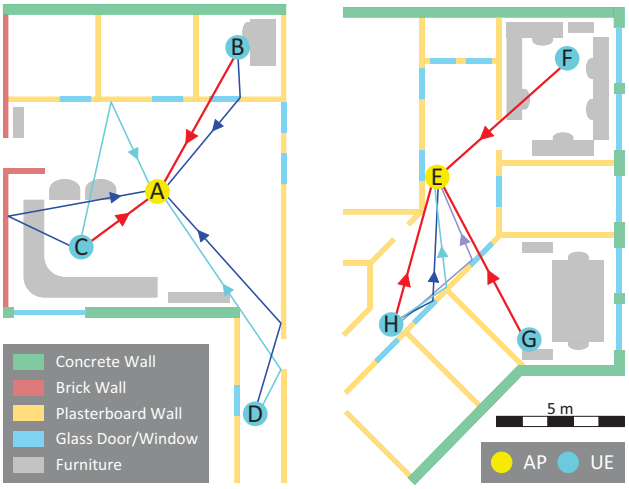

Fig. 3: Indoor measurement locations showing the 60 GHz AP–UE links (LOS links: red; NLOS links: blue).

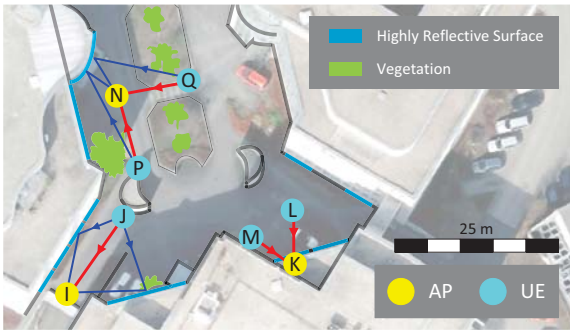

Fig. 4: Outdoor measurement locations showing the 60 GHz AP–UE links (LOS links: red; NLOS links: blue).

A. 60 GHz Measurements and Link Determination

In Figs. 3 and 4, we present the feasible links, corresponding to the feasible AP–UE beam pairs, obtained from the 60 GHz measurement. The AP beams associated with each link for the different locations are shown using polar plots in Fig. 5. To determine the feasible links and the corresponding AP sectors between two 60 GHz nodes, we deployed 60 GHz USRP–SiversIMA packet-radio transceivers [11] as shown in Fig. 6. The transceivers are equipped with fixed directional antennas of beamwidth 10° and gain of 25 dBi, with the UE transmitting 60 GHz packets at 0 dBm. Given the fixed beams of our transceivers, we placed them on rotating turntables to enable easy steering of the beams through 360°, thereby emulating 36 virtual beams. The 60 GHz transceiver parameters are listed in Table III.

In principle, the actual feasible links between a given AP–UE node pair are determined by sequential scanning through all the AP–UE beam pairs and then selecting the set of feasible AP–UE beam pairs for which the RSS at the UE, $RSS_b > \lambda$. However, we note that for the IEEE 802.11ad beamsteering algorithm, the nodes do not always operate in directional mode, receiving quasi-omnidirectional during the

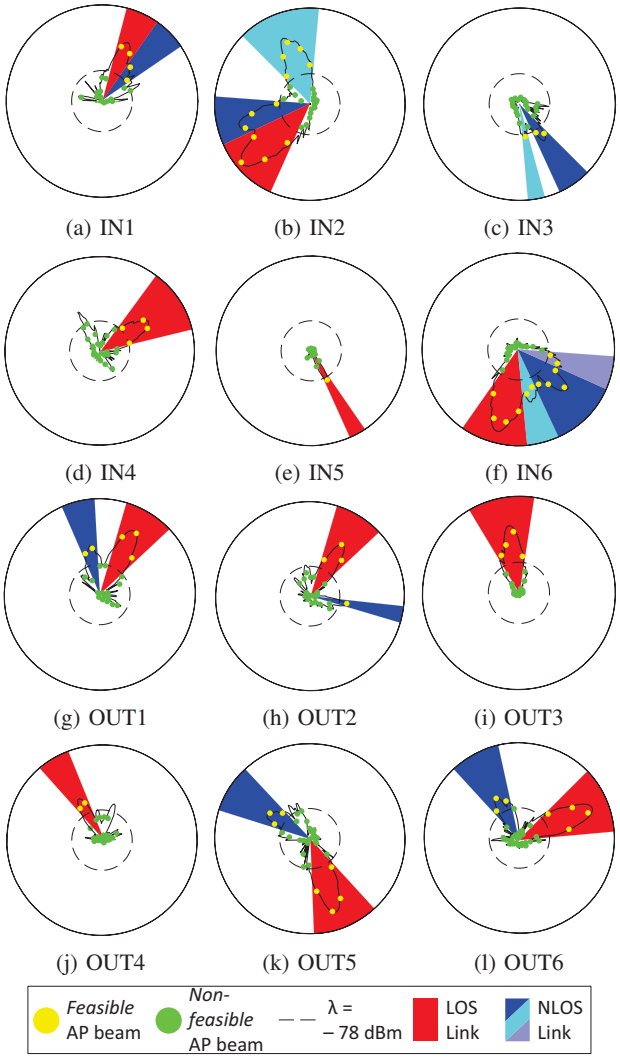

Fig. 5: Polar plot for RSS along different AP beams for the different locations. AP beams corresponding to the same feasible LOS/NLOS link (cf. Figs.3 and 4) are grouped together by background color.

SLS phase. Therefore, to consider the effects of reduced gain for quasi-omnidirectional reception in determining feasible AP–UE beams, we also estimated the quasi-omnidirectional reception RSS, RSS_o using our fixed beam antenna transceiver setup by substituting the directional receiver gain, G^b_{RX} from the measured RSS_b with a quasi-omnidirectional receiver gain, G^o_{RX}. Therefore, for every AP–UE beam pair we have a *measured* directional RSS, RSS_b and an *emulated* quasi-omnidirectional RSS, RSS_o. Following an exhaustive scanning, we determined the set of feasible AP–UE beams by comparing the RSS_o with $\lambda = -78$ dBm (chosen considering the IEEE 802.11ad control PHY threshold). We note that we employed RSS_o only to determine the detected feasible links, whereas RSS_b provides the real measure of the RSS at the UE for the eventually *established* link.

Once the feasible links between the nodes are determined, we extracted the feasible AP sectors associated with these

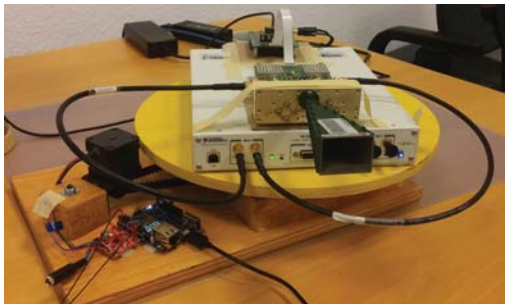

Fig. 6: 60 GHz USRP-SiversIMA transceiver with 10° beamwidth fixed beam horn antenna on a turntable.

TABLE III: 60 GHz MEASUREMENT PARAMETERS

Transmission Power	0 dBm
RX Sensitivity Threshold, λ	-78 dBm
Directional Antenna Beamwidth	10°
Directional Antenna Gain, $G^b_{RX} = G_{TX}$	25 dBi
Quasi-omnidirectional Antenna Gain, G^o_{RX}	10 dBi
(G^o can be maximum 15 dB less than G^b [4])	

links. Future mm-wave digital beamforming antennas will be able to generate both narrow beams and wider sectors by varying the antenna array weight vectors. However, our transceivers are equipped with a single fixed beam antenna of beamwidth 10°. Consequently, to determine feasible AP sectors and compare them with the AP sectors predicted by the 2.4 GHz AoA estimation system, we emulated sectors by virtually concatenating neighboring beams. As mentioned in Section IV, it is of interest to investigate the performance of *AoASteer* for antennas with a different number of sectors to understand the tradeoff between the feasible link discoverability and latency reduction. Our sector emulation model therefore further facilitated in considering different numbers of antenna sectors for the 36 virtual beams available, e.g., antennas with 3 sectors (12 beams per sector), 6 sectors (6 beams per sector), etc. Additionally, to evaluate the effects of random sector orientations, for each sector configuration we exhaustively considered all the different sector boundaries with respect to a reference orientation. For example, for a 3-sector node (12 beams per sector), we considered several sector boundaries, such as [0°-110°, 120°-230°, 240°-350°] and [90°-200°, 210°-330°, 340°80°], to evaluate *AoASteer*.

B. 2.4 GHz Measurements and AoA Estimation

For the 2.4 GHz measurements, a signal generator at the UE transmited a 20 dBm continuous wave signal at 2.484 GHz. To determine the AoA of the signal received at the AP, we employed a receiver with an 8-element uniform linear array (8-ULA) antenna developed in [12]. Each antenna element, with a gain of 3 dBi, is connected to an NI USRP running the AoA estimation algorithm implemented using GNU Radio. A linear antenna array is capable of detecting the AoA of the received signal for a 180° field of view only. Therefore, the AoA estimation accuracy of an ULA-based system is dependent on the antenna array orientation with respect to

Fig. 7: 2.4 GHz AoA estimation system receiver setup consisting of 8-element uniform linear array (8-ULA) antenna.

TABLE IV: 2.4 GHz MEASUREMENT PARAMETERS

Operational frequency	2.484 GHz (Ch.14–IEEE 802.11b/g/n)
Transmission Power	20 dBm
RX Antenna Config.	8-element uniform linear array

the transmitting node. To evaluate the performance of our 8-ULA AoA estimation system for random array orientations, we estimated the AoA for 36 different 8-ULA orientations (i.e., for every 10° covering 360°) at the AP, for each AP location. The 2.4 GHz AoA estimation setup is shown in Fig. 7 and the measurement parameters are listed in Table IV.

Our 2.4 GHz AoA estimation algorithm is based on the MUSIC algorithm with spatial smoothing and threshold-based peak classification. Based on the incoming 2.4 GHz signal, a MUSIC spectrum is generated for azimuth angle ϕ, varying over the complete 360° in the horizontal plane. Evaluated with a step size of $\Delta\phi$, the generated MUSIC spectrum $Z(\phi)$ produces multiple AoA peaks. We filter the AoA peaks based on a threshold value θ_{th}, calculated as

$$\theta_{th} = \mu + \alpha\sigma,\ \alpha \in \mathbb{R}^+, \tag{4}$$

where μ is the expected value, σ is the standard deviation of $Z(\phi)$, and α is a fixed real positive factor that determines the sensitivity of the peak classification. For our measurements, we set $\alpha = 1$. For every peak i, the values $\phi_{start,i}$ and $\phi_{end,i}$ give the boundaries of the MUSIC spectrum samples above θ_{th}. The algorithm computes the maxima of the MUSIC spectrum, $Z(\phi)$ within the boundary values and returns the angle $\hat{\phi}_i$ as an estimated signal AoA. Considering the complete MUSIC spectrum, the estimated AoA peaks are sorted in descending order of amplitude and stored in a vector $\hat{\boldsymbol{\phi}}$.

C. Beamsteering Algorithm Performance Metrics

1. Latency: Depending on the number of estimated AP sectors, $|\mathbf{m}|$, and the estimation accuracy, we calculate the link establishment latency of *AoASteer* using (2) and (3). The *AoASteer* latency is compared with that of IEEE 802.11ad.

2. Link Quality: *AoASteer* establishes a link by searching over a subset of estimated AP sectors, $\mathbf{m}$. Therefore, it may not always predict the best link between the nodes as is selected by the IEEE 802.11ad algorithm. We evaluate the established link quality by computing the difference in RSS at the UE for the links established by *AoASteer* and the IEEE 802.11ad algorithm. We further compute the achievable data rate for the established link by *AoASteer* and compare it with that of the IEEE 802.11ad algorithm by mapping the RSS of the links to the IEEE802.11ad autorate function/MCS table [4].

The link establishment latency and the link quality are determined for all the different locations, and number of sectors per node antenna, $|\mathbf{M}|$ = 2, 3, 4, 6, and 9 (for total 36 beams). For each value of $|\mathbf{M}|$ for a given AP-UE pair, we report the metric *distributions* computed considering all the 36 orientation of 8-ULA and all possible sector boundaries. We show these distributions in terms of boxplots showing the median, upper and lower quartile values, and whiskers at maximum 1.5 times interquartile range from the median.

VI. Results and Performance Analysis

In this section, we first present the 60 GHz AP sector prediction results of our 2.4 GHz AoA estimation system, followed by the performance evaluation results of *AoASteer* against that of the IEEE 802.11ad beamsteering algorithm, presented in terms of the metrics in Section V-C.

A. AP Sector Estimation

In Fig. 8a we present the number of feasible AP sectors corresponding to the feasible 60 GHz links for different number of sectors per AP antenna, $|\mathbf{M}|$, and different measurement locations. Given that we consider several sector boundaries, the number of feasible AP sectors between the nodes vary for a given value of $|\mathbf{M}|$. Nevertheless, the total number of feasible links between the AP-UE pair remains the same. Fig. 8a shows that the number of feasible AP sectors increases with the increase in $|\mathbf{M}|$ as the feasible links are distributed across an increased number of AP sectors, e.g. the median feasible AP sectors at IN2 increases from 2 for $|\mathbf{M}| = 2$ to 4.5 for $|\mathbf{M}| = 9$. Overall, a median of 2 feasible AP sectors is available for $|\mathbf{M}| = 3$ to 9, except for $|\mathbf{M}| = 2$ where a median of 1 feasible AP sector is present. The number of feasible links also depend on the node locations, and therefore, the number of feasible AP sectors vary across locations. For example, while only 1 AP sector is available at IN5 for all values of $|\mathbf{M}|$, the feasible AP sectors increases from 2 ($|\mathbf{M}| = 2$) to 5 ($|\mathbf{M}| = 9$) at IN2.

In Figs. 8b and 8c, we present the number of feasible AP sectors discovered during the SLS phase of the IEEE 802.11ad beamsteering algorithm, and correctly predicted during the S-SLS phase of *AoASteer*, respectively. For the *AoASteer* evaluation, we consider only up to 3 estimated AP sectors (corresponding to the top three AoA peaks obtained from the MUSIC spectrum) and different orientations of the 2.4 GHz 8-ULA receiver to take into account the influence of random array orientations on AoA estimation. We also note that we consider different sector gains corresponding to the sector widths (i.e., sector gain proportional to $|\mathbf{M}|$) for our evaluation. Accordingly, during the SLS/S-SLS phases, not all the feasible AP sectors in Fig. 8a are discovered by the beamsteering algorithms. For example, Figs. 8b and 8c show that no feasible AP sector is discovered at IN3 and IN5 during neither the SLS nor the S-SLS phases for any value of $|\mathbf{M}|$, even though Fig. 8a shows that directional links do exist between the nodes at these locations. We further observe that for the IEEE 802.11ad beamsteering algorithm, a median of 1 feasible AP sector is discoverable for $|\mathbf{M}| = 2$ to 6, with 2 feasible AP sectors discoverable for $|\mathbf{M}| = 9$ only. In contrast, *AoASteer* is able to correctly estimate a median of 1 feasible AP sector for all values of $|\mathbf{M}|$. Given the increase in the number of feasible AP sectors with the increase in $|\mathbf{M}|$, the discoverability of AP sectors for the IEEE 802.11ad beamsteering algorithm increases likewise. However, this does not improve the AP sector estimation accuracy for *AoASteer*, as with the increase in the values of $|\mathbf{M}|$, the AP sector beamwidth decreases, thereby increasing the complexity of precisely mapping the AoA estimations to the AP sector. Comparing the indoor and outdoor performance, we note that the AP sector estimation accuracy of *AoASteer* is slightly better for indoor locations (especially for higher values of $|\mathbf{M}|$) compared to outdoors, given the presence of stronger reflective links indoors. For example, while *AoASteer* correctly predicts a median of 1 feasible AP sector for $|\mathbf{M}| = 9$ indoors, no feasible AP sectors are predicted for the outdoor locations.

Linear antenna arrays have a 180° field of view and consequently, estimate AoA accurately along selected array orientations only. Furthermore, a linear array often falsely produces the mirror image peaks corresponding to the actual AoAs in the MUSIC spectrum over 360°, leading to an increased number of false AP sector estimations. Mirror image detection by our 8-ULA severely affects the accuracy of our 2.4 GHz AoA estimation system. This issue can be tackled by instead using a uniform circular array (UCA) for AoA estimation. With a field of view of 360°, a UCA produces no mirror images for actual AoA peaks. Accordingly, to illustrate the improvements we expect from using a UCA, we emulate the AoA estimation results for a UCA-based receiver by filtering out the mirror images from the AoA estimation results produced by our 8-ULA system and present them in Fig. 8d. The UCA results show improved estimation accuracy, e.g., in locations IN6, OUT1 and OUT3 for the higher values of $|\mathbf{M}|$. Furthermore, considering all outdoor locations, the UCA-based estimator is able to correctly estimate a median of 1 feasible AP sector – an improvement over no feasible AP sector estimation in outdoor locations using our 8-ULA.

The results in Fig. 8 show that we can successfully predict feasible 60 GHz AP sectors through 2.4 GHz AoA estimation, with the median detection capability of *AoASteer* and the IEEE 802.11ad beamsteering algorithm being equal for $|\mathbf{M}| = 2$ to 6. Furthermore, in contrast to the default IEEE802.11ad SLS phase, these feasible AP sectors are estimated faster by *AoASteer* using S-SLS. Hence, we expect *AoASteer* to successfully

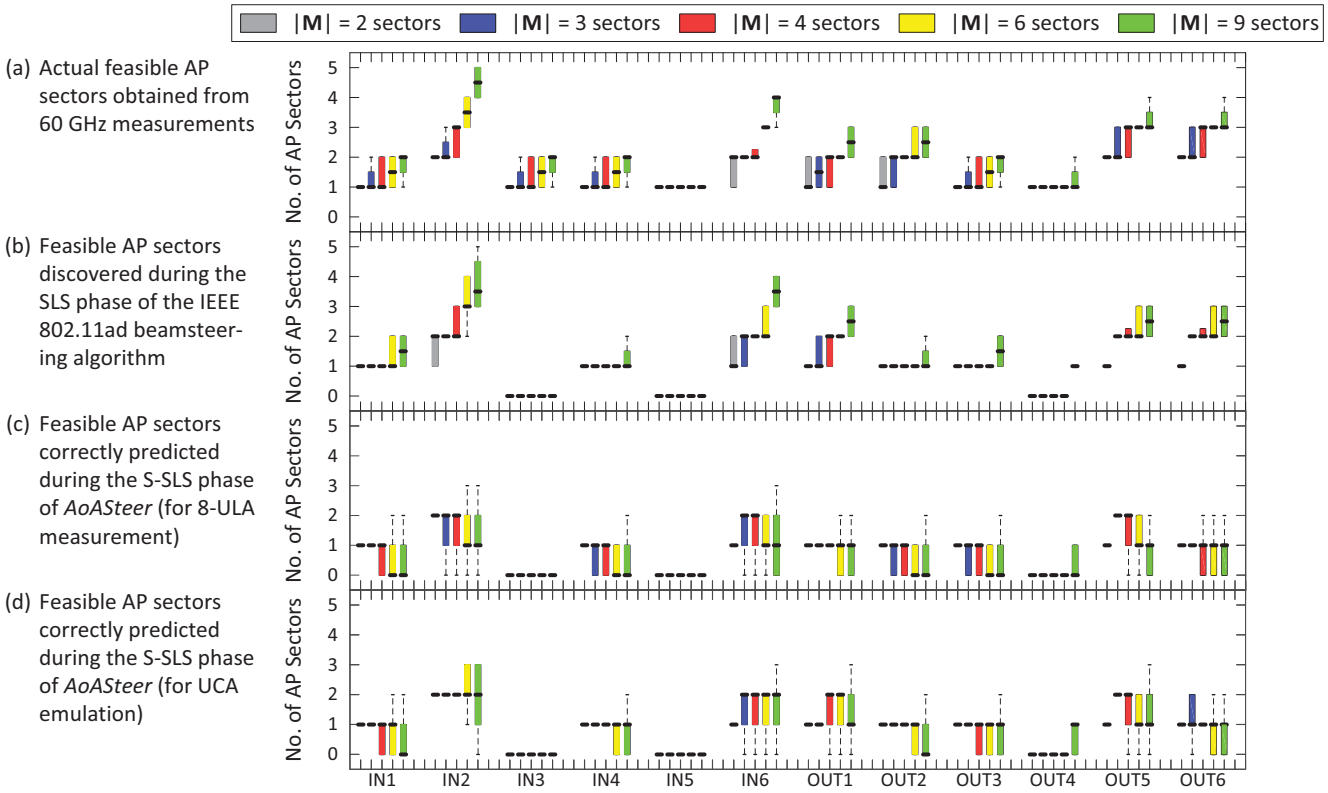

Fig. 8: Actual feasible AP sectors, feasible AP sectors discoverable by the IEEE 802.11ad beamsteering algorithm and feasible AP sectors correctly predicted by our 2.4 GHz AoA estimation system for different locations (cf. Table II) and values of $|\mathbf{M}|$.

establish a link between nodes at a lower latency as compared to the IEEE 802.11ad link beamsteering algorithm.

B. Link Establishment Latency

In Fig. 9, we present the latency results of *AoASteer* against that of IEEE802.11ad for measurements at locations in Figs. 3 and 4. As shown in Fig. 8, no link establishment is possible for IN3, IN5 and OUT (except for $|\mathbf{M}| = 9$); we thus exclude these locations from further results. Calculating the latency for $|\mathbf{m}| = 1, 2,$ and 3, we observe in Fig. 9 that with the increase in $|\mathbf{M}|$, the latency increases proportionally as the number of correctly predicted AP sectors decreases (see Figs. 8c and 8d). For $|\mathbf{m}| = 1$, the median *AoASteer* latency is 202.4 μs for $|\mathbf{M}| = 2$ and increases to 326.5 μs for $|\mathbf{M}| = 4$. Given the influence of the array orientation and mirror image detection on the estimation accuracy, for $|\mathbf{m}| = 1$ we achieve a median latency reduction of 19% compared to the IEEE 802.11ad latency for $|\mathbf{M}| = 2$ only. The results improve for $|\mathbf{m}|$ = 2 and 3, for which we observe a median latency of 199.9 μs and 215.7 μs for $|\mathbf{M}| = 4$, i.e. a 24% and 18% reduction respectively. For $|\mathbf{m}| = 2$, latency reduction is achieved for 84%, 74% and 64% of the overall measurement cases for all the locations considering $|\mathbf{M}| = 2, 3$ and 4 respectively. Considering $|\mathbf{m}| = 3$, *AoASteer* reduces latency for at least 50% of the overall cases for all values of $|\mathbf{M}|$. The performance varies somewhat according to locations, e.g. IN4 and OUT3 achieve no median latency reduction for $|\mathbf{M}|$ greater than 4 due to the availability of few feasible AP sectors, which reduces the chance of accurately estimating AP sectors especially for higher values of $|\mathbf{M}|$. Comparing indoors and outdoors, we observe higher latency reduction indoors given the presence of stronger reflective links that may be chosen over the primary link by *AoASteer*. For $|\mathbf{M}| = 6$ and $|\mathbf{m}| = 2$, latency reduction is achieved for 77% of the indoor cases, but only for 70% of the outdoors cases.

We expect to further reduce latency by using a UCA for AoA estimation, thereby avoiding the detection of false mirror images and the dependence on array orientation. To estimate the expected latency reduction, we present the results for our emulated UCA-based AoA estimation (for $|\mathbf{m}|$ = 3) in Fig. 10. We observe that UCA achieves latency reduction for a significantly higher number of cases compared to the 8-ULA. For $|\mathbf{M}| = 3$ and 6, UCA reduces latency for 89% and 75% of the overall cases respectively, compared to latency reduction for 82% and 61% of the time for our 8-ULA in Fig. 9.

C. Quality of Established Links

The results in Section VI-B show that our 8-ULA implementation achieves significant latency reduction, reducing latency for 50%-84% of the overall cases for $|\mathbf{m}|$ = 3. Thus, for the sake of brevity, we present the further results for $|\mathbf{m}| = 3$ and 8-ULA only. Fig. 11 presents the difference in the RSS at the UE for the links selected by *AoASteer* and the IEEE 802.11ad beamsteering algorithm at different locations.

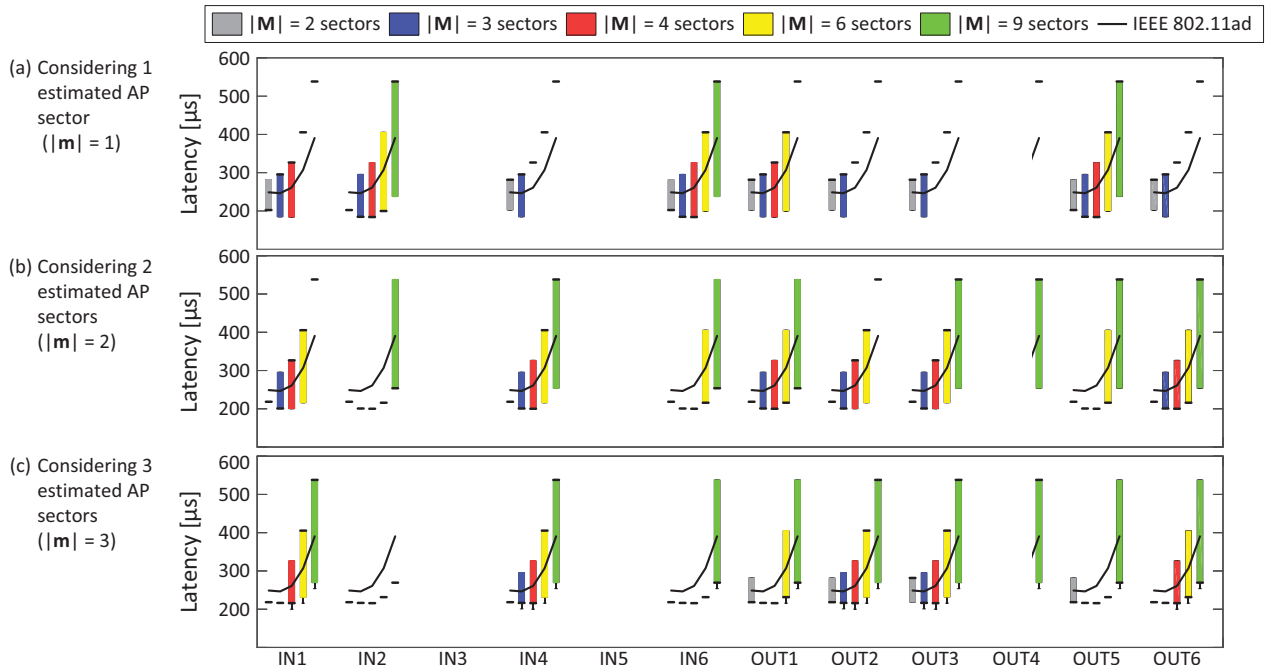

Fig. 9: Link establishment latency using *AoASteer* for different locations (cf. Table II), number of estimated AP sectors, $|\mathbf{m}|$ and number of antenna sectors per node, $|\mathbf{M}|$.

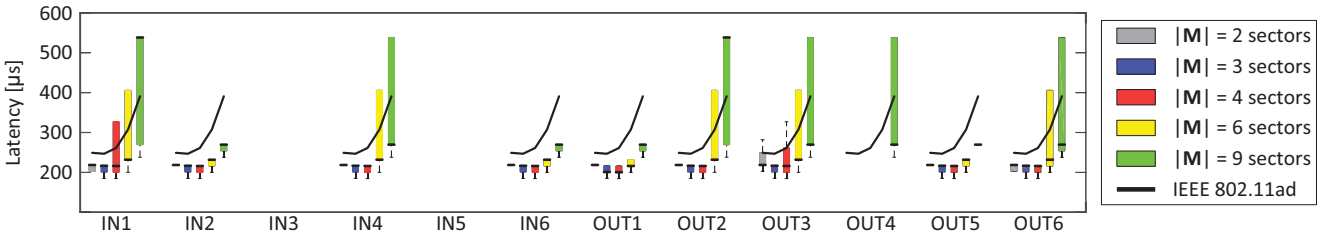

Fig. 10: Link establishment latency using *AoASteer* (number of estimated AP sectors, $|\mathbf{m}| = 3$) for different locations (cf. Table II) and number of antenna sectors per node, $|\mathbf{M}|$. An emulated UCA is employed for 2.4 GHz AoA estimation.

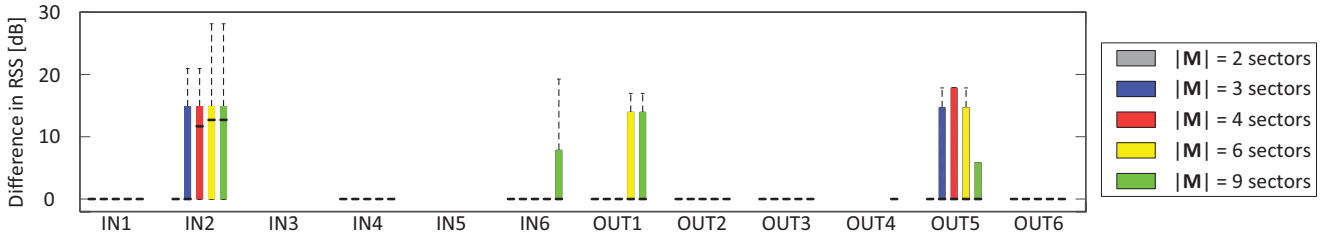

Fig. 11: Difference in RSS at the UE for the links established via *AoASteer* (number of estimated AP sectors, $|\mathbf{m}| = 3$) and the IEEE 802.11ad beamsteering algorithm for different locations (cf. Table II) and number of antenna sectors per node, $|\mathbf{M}|$.

A difference in RSS is observed when *AoASteer* selects a non-optimal, secondary link over the best link between two nodes to speed up link establishment. The RSS difference increases with the increase in $|\mathbf{M}|$; this is because for a higher value of $|\mathbf{M}|$, the sector width decreases, thereby making it more difficult for our AoA estimation system to precisely select the best feasible AP sector. For example, Fig. 12 shows that *AoASteer* achieves a median RSS difference of 0 dB for $|\mathbf{M}| = 2$ and 3, whereas for $|\mathbf{M}| = 4$ to 9 the median RSS difference is over 11 dB, indicating preferential selection of a secondary link over the primary link. Nevertheless, *AoASteer* is able to select the best link for 98% of the overall cases for $|\mathbf{M}| = 2$. Even for the worst case, i.e. for $|\mathbf{M}| = 9$, the best link is selected for 79% of the overall cases. Comparing the indoor and the outdoor locations, we observe that the best link is more often selected outdoors, given the availability of stronger NLOS links indoors as an alternative to the primary link. For $|\mathbf{M}| = 6$, while the best link is selected for 83% of

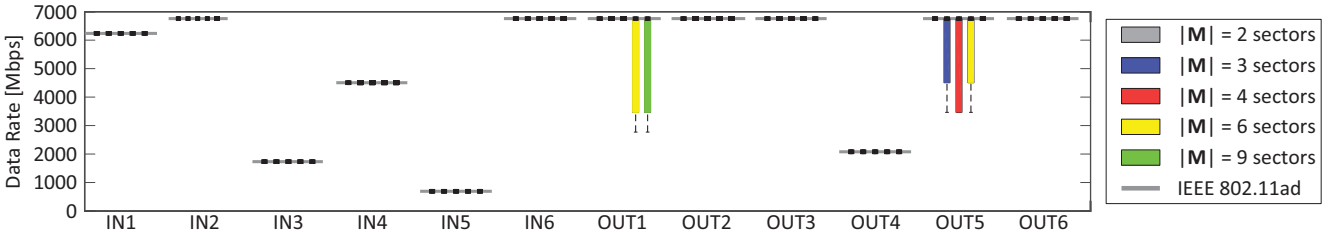

Fig. 12: Data rate achieved for the links established using *AoASteer* (number of estimated AP sectors, $|\mathbf{m}| = 3$) for different locations (cf. Table II) and number of antenna sectors per node, $|\mathbf{M}|$.

the outdoor cases, it is chosen for 77% of the indoor cases.

The data rate achieved by a link depends on the RSS. Accordingly, in Fig. 12 we present the achievable data rate for the links established via *AoASteer* and the IEEE 802.11ad beamsteering algorithm, calculated considering the OFDM PHY data rates in the IEEE 802.11ad standard [4], for $|\mathbf{m}| = 3$ and the different locations. As a result of an exhaustive scanning, the optimal links selected by the IEEE 802.11ad algorithm always attain the highest achievable data rate. In comparison, while *AoASteer* achieves the highest data rate for 99% of the overall cases for $|\mathbf{M}| = 2$, the highest data rate is achieved for only 88% of the overall cases for $|\mathbf{M}| = 9$ owing to the increased likelihood of our AoA estimation system selecting a secondary link over the primary link for higher values of $|\mathbf{M}|$. Comparing indoors and outdoors, we see that even though a higher percentage of the best links are chosen for outdoors, the highest data rate is more often achieved by indoor links. This is a consequence of the presence of stronger secondary links indoors that ensure higher RSS and thereby, a higher data rate at the UE compared to the outdoor secondary links. For example, most of the chosen secondary links at IN2 achieve the highest data rate of 6.7 Gbps as also achieved by the primary link. For OUT1 and OUT5, even though fewer non-optimal links are chosen, none of these secondary links achieve the highest data rate. Consequently, while the highest data rate is achieved for 72% and 82% of the measurement cases only for $|\mathbf{M}| = 9$ at OUT1 and OUT3, it is achieved for 85% of the measurement cases at IN2. From these results, we conclude that even though *AoASteer* does not always attain the highest achievable data rate, nonetheless the links selected by *AoASteer* provide multi-Gbps connectivity between the nodes, with a substantially reduced link establishment latency.

VII. Conclusions

In this paper we presented *AoASteer*, a 2.4 GHz-enhanced beamsteering algorithm for IEEE802.11ad mm-wave WLANs in which 2.4 GHz AoA estimates are used to predict 60 GHz AP sectors for fast link establishment. Our 2.4 GHz AoA estimation system with an 8-element ULA successfully estimates 60 GHz AP sectors to establish connectivity via both LOS and NLOS links. We experimentally evaluated *AoASteer* through extensive measurements in different indoor and outdoor locations, and considering different numbers of estimated AP sectors, $|\mathbf{m}|$, and antenna sectors per node, $|\mathbf{M}|$. Our results show that *AoASteer* correctly predicts a median of 1-2 feasible AP sectors (considering different measurement locations) using our 8-ULA based 2.4 GHz AoA estimation system. While the estimation accuracy is significantly reduced due to the mirror AoA peak detection in a linear antenna array with a 180° field of view, our results with an emulated circular array show a better estimation accuracy, given the UCA's 360° field of view that prevents mirror peak detection. To lessen the effects of false AP sector predictions for our present system, we considered $|\mathbf{m}| > 1$, i.e., more than one estimated AP sector for link establishment. Compared to IEEE 802.11ad, *AoASteer* reduces the link establishment latency by 30 μs and 120 μs for $|\mathbf{M}| = 2$ and 9 respectively, estimating three AP sectors (i.e., $|\mathbf{m}| = 3$) in the S-SLS phase. Furthermore, this latency reduction is achieved for 84% and 50% of the overall cases, respectively, while achieving the highest data rate for 99% and 88% of all the established links. Our results also show that even though non-optimal links are chosen more often indoors, *AoASteer* performs better indoors as compared to outdoors, given the presence of stronger secondary reflected links indoors.

References

[1] T. Nitsche *et al.*, "Steering with eyes closed: mm-Wave beam steering without in-band measurement," in *Proc. IEEE INFOCOM*, Apr. 2015.

[2] A. Patra *et al.*, "Smart mm-wave beam steering algorithm for fast link re-establishment under node mobility in 60 GHz indoor WLANs," in *Proc. ACM MobiWac*, Nov. 2015, pp. 53–62.

[3] S. Collonge *et al.*, "Influence of the human activity on the propagation characteristics of 60 GHz indoor channels," in *Proc. IEEE VTC*, vol. 1, Apr. 2003, pp. 251–255.

[4] *IEEE Standard: IEEE 802.11ad WLAN Enhancements for Very High Throughput in the 60 GHz Band*, Std., 2012.

[5] S. Sur *et al.*, "Beamspy: Enabling robust 60 GHz links under blockage," in *Proc. USENIX NSDI*, Mar. 2016, pp. 193–206.

[6] ——, "Scoping environment to assist 60 GHz link deployment," in *Proc. ACM MobiCom*, Sep. 2015, pp. 281–283.

[7] O. Abari *et al.*, "Millimeter wave communications: From point-to-point links to agile network connections," in *Proc. ACM HotNets*, Nov. 2016, pp. 169–175.

[8] K. Chandra *et al.*, "CogCell: Cognitive interplay between 60GHz picocells and 2.4/5GHz hotspots in the 5G era," *IEEE Commum. Mag.*, vol. 53, no. 7, pp. 118–125, 2015.

[9] E. M. Mohamed *et al.*, "WiFi assisted multi-WiGig AP coordination for future multi-Gbps WLANs," in *Proc. IEEE PIMRC*, Aug. 2015.

[10] C. Balanis, *Antenna Theory: Analysis and Design*. Wiley, 2005.

[11] J. Arnold *et al.*, "Demo: Spectrum-agile mm-wave packet radio implementation on USRPs," in *Proc. ACM SRIF*, Sep. 2015, pp. 5–8.

[12] S. Biehl, "Empirical Performance Evaluation of Angle-of-Arrival Estimation for Supporting Directional Wireless Links," Master's thesis, iNETS, RWTH Aachen University, Germany, 2015.